ELSEVIER

Colloids and Surfaces A: Physicochem. Eng. Aspects 229 (2003) 1–8

COLLOIDS AND SURFACES A

www.elsevier.com/locate/colsurfa

Large-pore mesoporous silica spheres: synthesis and application in HPLC

Yurong Ma, Limin Qi*, Jiming Ma, Yongqing Wu, Ou Liu, Humin Cheng

College of Chemistry, Peking University, Beijing 100871, PR China

Received 15 March 2003; accepted 13 August 2003

Abstract

Large-pore mesoporous silica microspheres with tailored pore sizes were prepared via a two-step synthesis process by using a triblock copolymer $EO_{20}PO_{70}EO_{20}$ as template in combination with a cosurfactant cetyltrimethylammonium bromide (CTAB) and a cosolvent ethanol. The obtained mesoporous silica spheres were characterized by scanning electron microscopy (SEM), transmission electron microscopy (TEM), X-ray diffraction (XRD), and N_2 sorption. The pore size of the silica spheres was increased up to 9.8 nm with increasing the hydrothermal treatment temperature in the second step to 130 °C. The presence of the cosolvent ethanol was found to be essential to the formation of mesoporous silica with a perfectly spherical morphology. Spherical mesoporous silica was successfully functionalized by dimethyloctadecylchlorosilane (C_{18}), leading to the formation of a C_{18}-modified spherical mesoporous silica. It has been shown that the C_{18}-modified mesoporous silica microspheres can be used as a good packing in high performance liquid chromatography (HPLC) to separate both small aromatic molecules and large biomolecules such as proteins.

Keywords: Mesoporous silica; Spheres; Triblock copolymer; HPLC; Proteins

1. Introduction

Since the discovery of M41S materials in 1992 [1,2], the synthesis of mesoporous silica with controlled nanostructures and macroscopic morphologies has received much attention owing to their potential applications in catalysis, separation, drug delivery, and nanocomposites [3–6]. Compared with traditional cationic and non-ionic surfactants, amphiphilic triblock copolymers have been used as very effective templates for the synthesis of ordered large-pore (up to 50 nm) mesoporous silica such as SBA-15 [7,8]. Many recent efforts have been devoted to the synthesis of mesoporous silica spheres of defined size and pore diameter because the control of the particle morphology and pore size of mesoporous silica could open up new possibilities for its application as a packing material in chromatography or as an easy-to-handle form for catalytic purposes [9–24]. Micrometer-sized mesoporous silica spheres can be used as chromatography stationary phases, in which crucial parameters are high surface area, well-defined pore size and uniform particle size. Commercial chromatography silica stationary phases usually exhibit

* Corresponding author. Tel.: +86-10-62751722; fax: +86-10-62751708.
E-mail address: liminqi@chem.pku.edu.cn (L. Qi).

0927-7757/$ – see front matter © 2003 Elsevier B.V. All rights reserved.
doi:10.1016/j.colsurfa.2003.08.010

lower surface area (less than 500 m^2/g), which is provided by inter-particle porosity, and larger pore size distribution; therefore, spherical mesoporous silica in micrometer scale has been reported as packing materials in chromatography [14,15]. Although a variety of micrometer-sized mesoporous silica spheres, which are suitable for application in high performance liquid chromatography (HPLC), have been synthesized, most of them were prepared using traditional surfactants as templates and so the pore sizes are usually less than 4 nm [12–15,18,19,21,22]. For the effective separation of biomacromolecules such as proteins, mesoporous silica spheres with larger pores would be more desirable. It is noteworthy that Zhao and co-workers [25–27] have synthesized large-pore (up to 8.1 nm) mesoporous SBA-15 with nearly spherical morphologies by using a triblock copolymer and a cosurfactant. These large-pore mesoporous SBA-15 particles have recently been functionalized by dimethyloctadecylchlorosilane ($CH_3(CH_2)_{17}Si(CH_3)_2Cl$; C_{18}) and applied as stationary phase in HPLC to separate large biomolecules [26,27]. However, it remains a challenge to synthesize large-pore mesoporous silica particles with a perfectly spherical morphology and tailored pore size.

Herein, large-pore (up to 9.8 nm) mesoporous silica spheres ranging in diameter from 3 to 6 μm have been obtained via a two-step synthesis process by using a triblock copolymer as template in combination with a cosurfactant and a cosolvent. By surface functionalization with C_{18}, the mesoporous silica microspheres can be used as a good packing in HPLC to separate both small aromatic molecules and large biomolecules such as proteins.

2. Experimental

2.1. Synthesis and functionalization of mesoporous silica spheres

Mesoporous silica spheres were synthesized by using tetraethyl orthosilicate (TEOS) as the silica source, poly(ethylene oxide)–block–poly(propylene oxide)–block–poly(ethylene oxide) (Aldrich, M_{av} = 5800, $EO_{20}PO_{70}EO_{20}$, P123) as the template, cetyltrimethylammonium bromide (CTAB) as the cosurfactant, and ethanol as the cosolvent. Typically, 0.3 g of triblock copolymer P123 and 0.05 g of CTAB were dissolved in a solution formed by mixing 6 ml of 2 M HCl, 3 ml H_2O and 2.5 ml ethanol. Then, 1 ml of TEOS was added in the aqueous solution at room temperature under magnetic stirring. The reactant molar ratio TEOS:P123:CTAB:HCl:EtOH:H_2O in the final reaction mixture was 1:0.011:0.031:2.67:9.18:116. After 30 min of stirring, the solution was transferred into a Teflon-lined steel Parr autoclave and heated at 80 °C for 5 h, and then kept at a higher temperature (120 or 130 °C) for 12 h. The white precipitate was recovered by filtration, dried at 90 °C for 24 h, and calcined in air at 550 °C for 5 h to remove the templates.

Dimethyloctadecylchlorosilane was used to functionalize the mesoporous silica spheres according to a previously reported method [26,27]. At first, 0.5 g dimethyloctadecylchlorosilane was dissolved in 30 ml toluene. Then, 0.5 g mesoporous SiO_2 spheres obtained after reacting at 80 °C for 5 h and then 120 °C for 12 h were added and the mixture was stirred for 24 h at room temperature. The C_{18}-modified product was recovered by filtration, washed with toluene thoroughly, and dried at 90 °C.

2.2. Characterization of mesoporous silica spheres

Scanning electron microscopy (SEM) images were taken on an AMARY 1910 field emission microscope. Transmission electron microscopy (TEM) images were obtained on a JEOL JEM-200CX microscope operating at 160 kV. Powder X-ray diffraction (XRD) patterns were measured on a Rigaku Dmax-2000 diffractometer using Cu Kα radiation. N_2 adsorption–desorption isotherms were determined on a Micromeritics ASAP-2010 apparatus. Prior to the measurement, the samples were heated at 220 °C for 3 h to remove water in the silica completely. For the functionalized mesoporous silica, infrared (IR) spectrum was measured with a Vector 22 FT-IR spectrophotometer and elementary analysis was performed by an Elementar Vario EL.

2.3. Separation of aromatic molecules and proteins with HPLC

An Agilent 1100 HPLC system composed of vacuum degasser, quaternary pump, Rheodyne 7725i

injector with 10 μl sample loop, variable wavelength detector (VWD) was used to determine the separation property of the C_{18}-modified silica spheres as a stationary phase. The C_{18}-modified silica spheres were slurry-packed into a 5 cm × 0.46 cm i.d. stainless steel column under pressure of 6000 psi (1 psi = 6896 Pa). Three aromatic molecules, naphthalene, biphenyl, and phenanthrene, were separated on the column using a water/methanol mixture (30/70, v/v) as the mobile phase of 0.5 ml/min with a wavelength detector at 254 nm. Three kinds of proteins, lysozyme (LYS, Biozyme, M = 14,300), human serum albumin (HSA, Sigma, M = 66,460), and bovine serum albumin (BSA, Sigma, M = 66,400), were also separated on the column using a water (0.1% TFA)/CH_3CN (0.1% TFA) mixture as the mobile phase with an eluant flow of 0.5 ml/min with a wavelength detector at 280 nm.

3. Results and discussion

3.1. Unmodified mesoporous silica spheres

Fig. 1 shows typical SEM images of mesoporous silica products obtained at different heat-treatment conditions. As shown in Fig. 1a, the sample obtained at 80 °C for 5 h (SiO_2-1) exhibited a perfectly spherical morphology with diameters ranging from 3 to 6 μm. When the SiO_2-1 microspheres were further heated at 120 °C (SiO_2-2) or 130 °C (SiO_2-3) for 12 h, the resulting products essentially kept the original morphology and size (Fig. 1b and c). It indicated that silica spheres formed when heated at 80 °C for 5 h, and the second heating step (at 120 or 130 °C) had no considerable effect on the macroscopic morphology and size. For comparison purpose, a silica sample (SiO_2-4) was prepared via a one step synthesis by directly heating the reaction mixture at 130 °C for 12 h, and it exhibited only irregular morphologies (Fig. 1d), indicating that the first heating step is essential to the formation of silica product with a spherical morphology.

To examine the effect of ethanol on the morphology of the product, a synthesis was performed in the absence of ethanol with other reaction conditions kept similar to that for SiO_2-3. The resulting product exhibited a mixture of lots of irregular particles and some microspheres (Fig. 2). The addition of the cosolvent ethanol may decrease the polarity of the solvent and thus decrease the rate of nucleation and growth of the mesostructured products because of the slower TEOS hydrolysis and mesostructure assembly, which could contribute to the formation of silica spheres

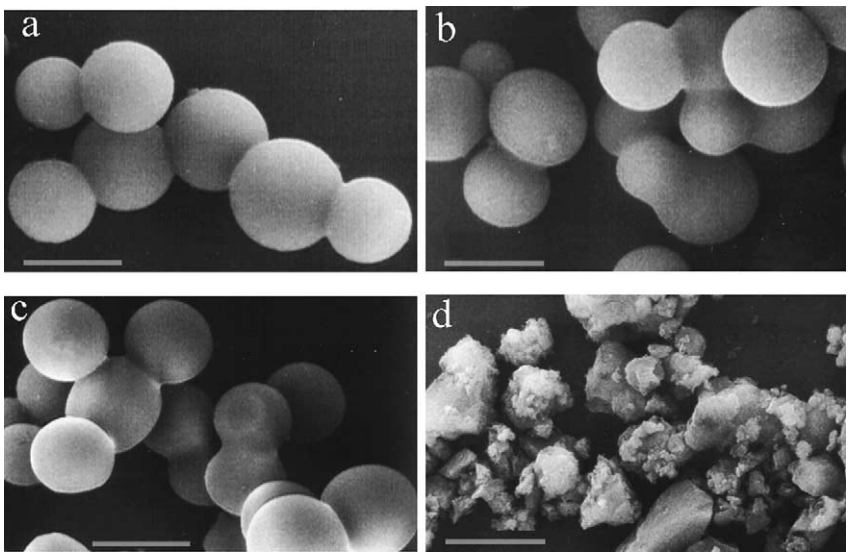

Fig. 1. SEM images of mesoporous SiO_2 obtained at: (a) 80 °C for 5 h (SiO_2-1); (b) 80 °C for 5 h and 120 °C for 12 h (SiO_2-2); (c) 80 °C for 5 h and 130 °C for 12 h (SiO_2-3); (d) 130 °C for 12 h (SiO_2-4). Scale bar: 5 μm.

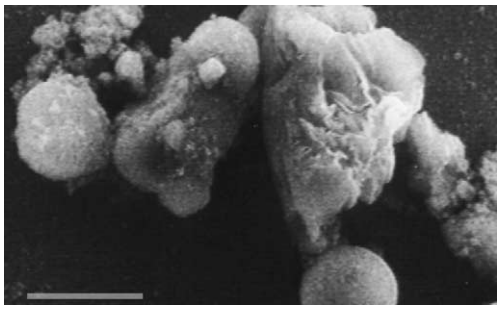

Fig. 2. SEM image of mesoporous SiO_2 synthesized in the absence of ethanol and under otherwise the same conditions as that of SiO_2-3. Scale bar: 5 μm.

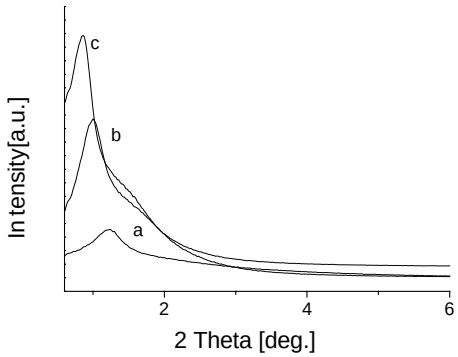

Fig. 3. XRD patterns of mesoporous silica spheres: (a) SiO_2-1; (b) SiO_2-2; (c) SiO_2-3.

with smooth surfaces. It has been reported that uniform mesoporous silica microspheres can be obtained by using alkylamine as a template and ethanol as an auxiliary solvent and a remarkable improvement of the spherical morphology has been attributed to the presence of ethanol [19]. It is noted that mesoporous SBA-15 particles obtained by using P123 as the template and CTAB as the cosurfactant did not show a perfectly spherical morphology [25–27], which suggested that the cosolvent ethanol played an important role in the formation of perfect spheres of mesoporous silica.

Small angle XRD patterns of the obtained mesoporous SiO_2 spheres were shown in Fig. 3, which shows that SiO_2-1, SiO_2-2, and SiO_2-3 exhibited single diffraction peaks with *d* spacings 7.3, 9.5, and 10.5 nm, respectively, characteristic of mesoporous materials with a pore structure lacking long-range order. The *d* spacing increased with increasing temperature in the second heating step, indicating that when heated at higher temperatures, the inner pore size of the preformed mesoporous silica spheres expanded while their exterior morphology and size kept unchanged.

N_2 adsorption–desorption isotherms and the corresponding BJH pore size distribution curves of the mesoporous silica spheres are shown in Fig. 4. As shown in Fig. 4a, all the samples exhibited type IV isotherms with well-defined steps associated with the filling of the mesopores due to capillary condensation. The pore size profiles for SiO_2-1, SiO_2-2, and SiO_2-3 displayed peaks as 4.3, 7.4, and 10.7 nm, respectively. The calculated average pore sizes for the three silica samples are 3.5, 6.6, and 9.8 nm, respectively, which is consistent with the XRD result. It has been documented that the pore size of mesoporous silica obtained by using triblock copolymer as template became larger at higher hydrothermal reaction temperature [28]. Therefore, the pore size of the mesoporous

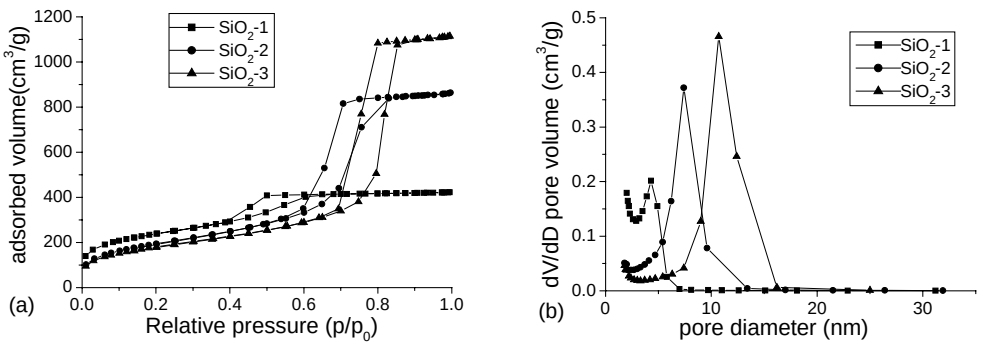

Fig. 4. N_2 adsorption–desorption isotherms (a) and pore size distribution curves from the adsorption branch (b) of mesoporous silica spheres.

Table 1
Physicochemical properties of mesoporous silica spheres

Sample code	Reaction conditions	d (nm)	Pore size (nm)	Pore volume (cm^3/g)	BET surface area (m^2/g)
SiO_2-1	80 °C for 5 h	7.3	3.5	0.58	853
SiO_2-2	80 °C for 5 h and 120 °C for 5 h	9.5	6.6	1.35	713
SiO_2-3	80 °C for 5 h and 130 °C for 5 h	10.5	9.8	1.74	660
SiO_2-2-C_{18}	80 °C for 5 h and 120 °C for 5 h, C_{18} functionalized	9.5	6.1	1.06	522

silica spheres can be easily adjusted by changing the hydrothermal treatment temperature in the second synthesis step. The physicochemical properties of the obtained mesoporous silica spheres were summarized in Table 1. It is noted that the pore volumes for SiO_2-2 and SiO_2-3 were 1.35 and 1.74 cm^3/g, respectively, much higher than those for the reported mesoporous SBA-15 particles (1.05 cm^3/g) [26,27].

A typical high-resolution TEM image of the SiO_2-2 spheres is presented in Fig. 5, which shows irregularly aligned mesopores with relatively uniform pore sizes (about 6–7 nm). This result is in good agreement with the related XRD and N_2 adsorption results. It has been documented that mesoporous silica with a hexagonal structure can be prepared via the co-assembly of either CTAB or P123 with cationic silica species in acid conditions [3,8]. Our preliminary results have shown that mesoporous silica products obtained in the presence of single CTAB or P123 under the current synthesis conditions have not exhibited the spherical morphology, suggesting that the presence of both CTAB and P123 is essential for the formation of the mesoporous silica spheres. In the present synthesis, the molar ratio between CTAB and P123 is about 3 but the weight ratio between them is actually very low (1/6). Therefore, the polymer P123 contributes largely to the final mesopores whereas the surfactant CTAB mainly plays a role of cosurfactant. The fact that the mesoporous silica obtained by using the mixed P123–CTAB templates shows a monodisperse rather than a bimodal pore size distribution indicates that the mesopores could be formed by the co-assembly of the mixed P123–CTAB micelles with cationic silica species (Fig. 6). Since the mixed P123–CTAB micelles are not so uniform as the single P123 or CTAB micelles, the final mesopore structure tends to lack a long-range hexagonal order.

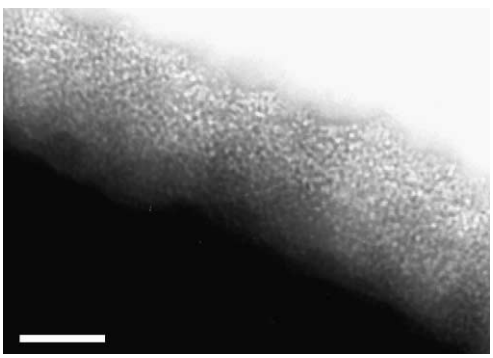

Fig. 5. TEM image of mesoporous silica spheres SiO_2-2. Scale bar: 100 nm.

3.2. C_{18}-modified mesoporous silica spheres and their application in HPLC

By the surface functionalization of mesoporous silica spheres SiO_2-2 with C_{18}, a C_{18}-modified

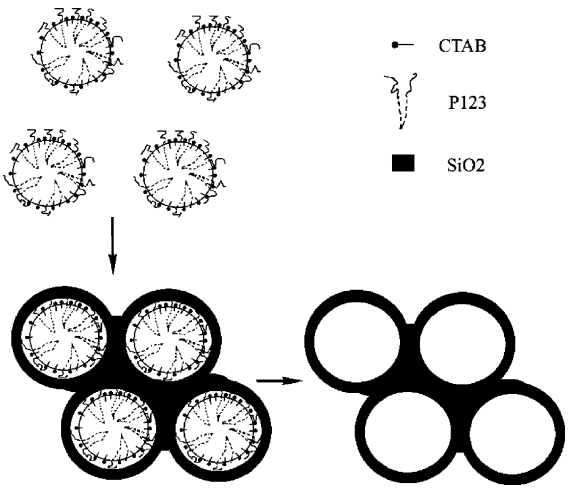

Fig. 6. Schematic diagram showing the assembly of the mixed P123–CTAB micelles and the formation of the final mesopore structure.

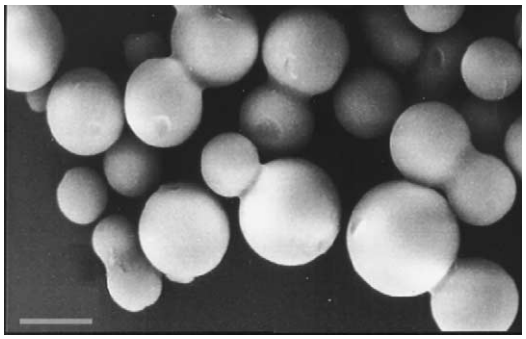

Fig. 7. SEM image of functionalized mesoporous silica spheres SiO_2-2-C_{18}. Scale bar: 5 μm.

mesoporous silica sample SiO_2-2-C_{18} was obtained. Fig. 7 presents a typical SEM image of SiO_2-2-C_{18}, which shows that it kept the spherical morphology for SiO_2-2. The IR spectrum of SiO_2-2-C_{18} shown in Fig. 8a exhibited two peaks at 2926 cm^{-1} (asymmetrical stretching, CH_2) and 2854 cm^{-1} (symmetrical stretching, CH_3), which is similar to that for mesoporous silica spheres functionalized by octyldimethylchlorosilane (C_8) [24], confirming the existence of C_{18} in the pores of the silica spheres. The peak at 3500–3000 cm^{-1} was adsorption of Si–OH at the surface of silica spheres. Elementary analysis revealed that the C content in SiO_2-2-C_{18} was 7.6%, and the molar ratio of Si to C_{18} in SiO_2-2-C_{18} was calculated to be 1:0.0232. The small angle XRD spectrum of SiO_2-2-C_{18} (Fig. 8b) showed just a shoulder rather than the sharp peak for SiO_2-2, which could be attributed to the existence of organic moieties due to the C_{18} modification on the pore surface of SiO_2-2.

Fig. 9 presents the adsorption–desorption isotherm of SiO_2-2-C_{18}, which was similar to that for SiO_2-2 generally. However, the average pore size decreased slightly from 6.6 to 6.1 nm and the BET surface area decreased considerably from 713 to 522 m^2/g, confirming that C_{18} was coupled with the inner pore surface of mesoporous SiO_2 spheres.

The obtained SiO_2-2-C_{18} microspheres were slurry-packed into an HPLC column for the separation of small aromatic molecules and biomacromolecules. For the separation of three aromatic molecules, a water/methanol mixture (30/70, v/v) was used as the mobile phase. Fig. 10a shows the separation chromatogram of three aromatic molecules obtained on the modified silica SiO_2-2-C_{18} column, which showed three well-separated, symmetric peaks corresponding to naphthalene, biphenyl, and phenanthrene, respectively. In contrast, the HPLC column packed with the unmodified silica SiO_2-2 spheres separated aromatic molecules poorly (inset of Fig. 10a), suggesting that functionalization of mesoporous silica spheres with C_{18} is essential to their successful application as an HPLC packing. It is noted that the orders of the separated solutes for the SiO_2-2 and SiO_2-2-C_{18} are reverse because the polarity of a silica surface is higher than that of the mobile phase (water/ethanol = 30/70, v/v) whereas the polarity of a C_{18}-modified silica surface is lower.

The separation result of proteins on the modified silica SiO_2-2-C_{18} column is shown in Fig. 10b, which exhibited three well-separated peaks corresponding to human serum albumin, lysozyme, and bovine serum

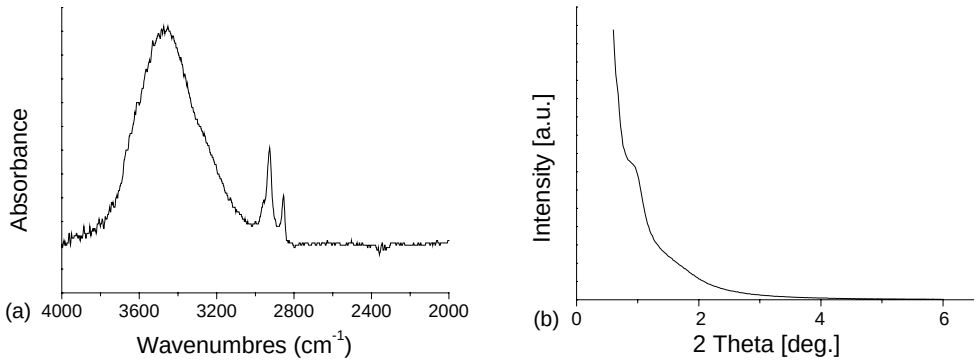

Fig. 8. IR (a) and XRD (b) spectra of functionalized mesoporous silica spheres SiO_2-2-C_{18}.

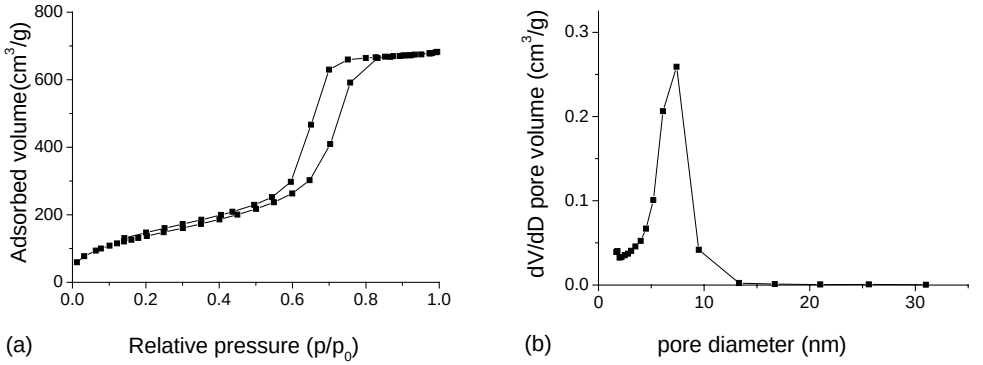

Fig. 9. N_2 adsorption–desorption isotherm (a) and pore size distribution curve from the adsorption branch (b) of functionalized mesoporous silica spheres SiO_2-2-C_{18}.

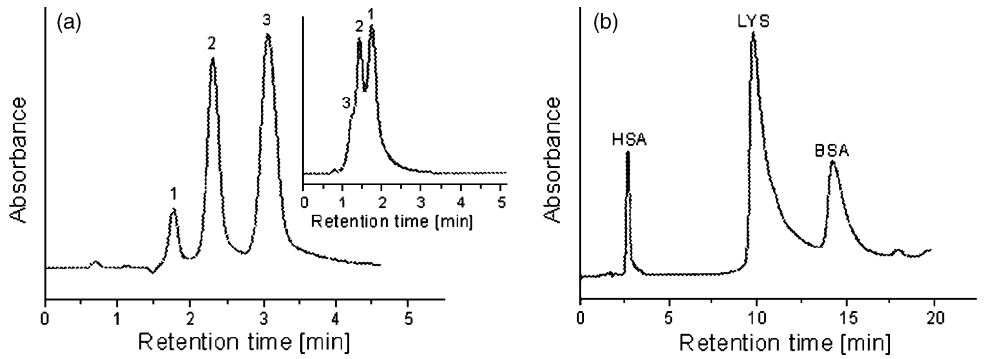

Fig. 10. Chromatograms of three aromatic molecules (a) and three proteins (b) with a SiO_2-2-C_{18} column. Inset in (a) shows chromatogram of aromatic molecules with a SiO_2-2 column. Peaks 1–3 in (a) correspond to naphthalene, biphenyl, and phenanthrene, respectively, whereas the three peaks in (b) correspond to human serum albumin (HSA), lysozyme (LYS), and bovine serum albumin (BSA), respectively.

albumin, respectively, indicating a nearly complete separation of the three large biomolecules. The relatively asymmetric peaks could be attributed to the non-uniform interspaces among the substrate spheres since the sizes of the mesoporous spheres were not uniform and some coagulation between the spheres occurred. Although the molecular weight of HSA (M = 66,460) is larger than LYS (M = 14,300), the retention time of the former is shorter, indicating that in addition to the effect of molecular sieving, the hydrophobic effect played an important role in determining the retention time [26]. In conclusion, the C_{18}-modified mesoporous silica microspheres SiO_2-2-C_{18} can be used as a good packing in HPLC to separate both small aromatic molecules and large biomolecules.

4. Conclusion

Large-pore mesoporous silica microspheres (3–6 μm) with tailored pore sizes were prepared via a two-step synthesis process by using a triblock copolymer $EO_{20}PO_{70}EO_{20}$ (P123) as template in combination with a cosurfactant CTAB and a cosolvent ethanol. The pore size of the silica spheres was increased up to 9.8 nm with increasing the hydrothermal treatment temperature in the second step to 130 °C. The presence of the cosolvent ethanol was found to be essential to the formation of mesoporous silica with a perfectly spherical morphology. Spherical mesoporous silica with a pore size of 6.6 nm (SiO_2-2) was successfully functionalized by dimethyloctadecylchlorosilane, leading to the formation of C_{18}-modified spherical

mesoporous silica (SiO_2-2-C_{18}) with a pore size of 6.1 nm. It has been shown that the SiO_2-2-C_{18} mesoporous silica microspheres can be used as a good packing in HPLC to separate both small aromatic molecules and large biomolecules such as proteins.

Acknowledgements

This work was supported by NSFC (20003001, 20233010) and the Special Fund for Authors of Chinese Excellent Doctoral Theses, MOE, China (200020).

References

[1] C.T. Kresge, M.E. Leonowicz, W.J. Roth, J.C. Vartuli, J.S. Beck, Nature 359 (1992) 710.
[2] J.S. Beck, J.C. Vartuli, W.J. Roth, M.E. Leonowicz, C.T. Kresge, K.D. Schmitt, C.T.-W. Chu, D.H. Olson, E.W. Sheppard, S.B. McCullen, J.B. Higginsand, J.L. Schlenker, J. Am. Chem. Soc. 114 (1992) 1083.
[3] J.Y. Ying, C.P. Mehnert, M.S. Wong, Angew. Chem. Int. Ed. 38 (1999) 56.
[4] A. Stein, B.J. Melde, R.C. Schroden, Adv. Mater. 12 (2000) 1403.
[5] A. Sayari, S. Hamoudi, Chem. Mater. 13 (2001) 3151.
[6] H.-P. Lin, C.-Y. Mou, Acc. Chem. Res. 35 (2002) 927.
[7] D.Y. Zhao, J.G. Feng, Q.S. Huo, N. Melosh, G.H. Fredrickson, B.F. Chmelka, G.D. Stucky, Science 279 (1998) 548.
[8] D.Y. Zhao, Q.S. Huo, J.G. Feng, B.F. Chmelka, G.D. Stucky, J. Am. Chem. Soc. 120 (1998) 6024.
[9] S. Schacht, Q. Huo, I.G. Voigt-Martin, G.D. Stucky, F. Schuth, Science 273 (1996) 768.
[10] Q. Huo, J. Feng, F. Schuth, G.D. Stucky, Chem. Mater. 9 (1997) 14.
[11] M. Grun, I. Lauer, K.K. Unger, Adv. Mater. 9 (1997) 254.
[12] L. Qi, J. Ma, H. Cheng, Z. Zhao, Chem. Mater. 10 (1998) 1623.
[13] H. Yang, G. Vovk, N. Coombs, I. Aokolov, G.A. Ozin, J. Mater. Chem. 8 (1998) 743.
[14] K.W. Gallis, J.T. Araujo, K.J. Duff, J.G. Moore, C.C. Landry, Adv. Mater. 11 (1999) 1452.
[15] C. Boissiere, M. Kummel, M. Persin, A. Larbot, E. Prouzet, Adv. Funct. Mater. 11 (2001) 129.
[16] L. Sierra, B. Lopez, J.-L. Guth, Microporous Mesoporous Mater. 39 (2000) 519.
[17] B. Pauwels, G.V. Tendeloo, C. Thoelen, W.V. Rhijn, P.A. Jacobs, Adv. Mater. 13 (2001) 1317.
[18] K. Kosuge, P.S. Singh, Microporous Mesoporous Mater. 44 (2001) 139.
[19] K. Kosuge, P.S. Singh, Chem. Mater. 13 (2001) 2476.
[20] J.L. Blin, A. Leonard, B.L. Su, Chem. Mater. 13 (2001) 3542.
[21] T. Martin, A. Galarneau, F. Di Renzo, F. Fajula, D. Plee, Angew. Chem. Int. Ed. 41 (2002) 2590.
[22] G.V.R. Rao, G.P. Lopez, J. Bravo, H. Pham, A.K. Datye, H.F. Xu, T.L. Ward, Adv. Mater. 14 (2002) 1301.
[23] R.I. Nooney, D. Thirunavukkarasu, Y. Chen, R. Josephs, A.E. Ostafin, Chem. Mater. 14 (2002) 4721.
[24] A. Matsumoto, K. Tsutsumi, K. Schumacher, K.K. Unger, Langmuir 18 (2002) 4014.
[25] D. Zhao, Q. Sun, G.D. Stucky, Chem. Mater. 12 (2000) 275.
[26] J.W. Zhao, F. Gao, Y.L. Fu, W. Jin, P.D. Yang, D.Y. Zhao, Chem. Commun. (2002) 752.
[27] G. Feng, J.W. Zhao, S. Zhang, F. Zhou, W. Jin, X.M. Zhang, P.Y. Yang, D.Y. Zhao, Chem. J. Chin. Univ. 23 (2002) 1494.
[28] A. Galarneau, H. Cambon, F. Di Renzo, F. Fajula, Langmuir 17 (2001) 8328.